

Fabrication of electroless nickel plated aluminum freeform mirror for an infrared off-axis telescope

SANGHYUK KIM,¹ SEUNGHYUK CHANG,^{2,*} SOOJONG PAK,¹ KWANG JO LEE,³ BYEONGJOON JEONG,^{1,4} GIL-JAE LEE,⁵ GEON HEE KIM,⁴ SANG KYO SHIN,⁶ AND SONG MIN YOO⁷

¹School of Space Research, Kyung Hee University, Yongin 446-701, South Korea

²Center for Integrated Smart Sensors, Seoul 135-854, South Korea

³Department of Applied Physics, College of Applied Science, Kyung Hee University, Yongin 446-701, South Korea

⁴Optical Instrumentation Team, Korea Basic Science Institute, Daejeon 169-148, South Korea

⁵Material Machining Team, Medical Device Development Center, Cheongwon 363-951, South Korea

⁶Yoonseul Inc., 80 Daehwa-ro 32-beon-gil, Daedeog-gu, Daejeon 34364, South Korea

⁷College of Engineering, Kyung Hee University, Yongin 446-701, South Korea

*Corresponding author: chang@offaxis.co.kr

Received 26 August 2015; revised 31 October 2015; accepted 2 November 2015; posted 3 November 2015 (Doc. ID 248373); published 25 November 2015

Freeform mirrors can be readily fabricated by a single point diamond turning (SPDT) machine. However, this machining process often leaves mid-frequency errors (MFEs) that generate undesirable diffraction effects and stray light. In this work, we propose a novel thin electroless nickel plating procedure to remove MFE on freeform surfaces. The proposed procedure has a distinct advantage over a typical thick plating method in that the machining process can be endlessly repeated until the designed mirror surface is obtained. This is of great importance because the sophisticated surface of a freeform mirror cannot be optimized by a typical SPDT machining process, which can be repeated only several times before the limited thickness of the nickel plating is consumed. We will also describe the baking process of a plated mirror to improve the hardness of the mirror surface, which is crucial for minimizing the degradation of that mirror surface that occurs during the polishing process. During the whole proposed process, the changes in surface figures and textures are monitored and cross checked by two different types of measurements, as well as by an interference pattern test. The experimental results indicate that the proposed thin electroless nickel plating procedure is very simple but powerful for removing MFEs on freeform mirror surfaces. © 2015 Optical Society of America

OCIS codes: (220.4610) Optical fabrication; (220.4840) Testing; (220.1920) Diamond machining; (220.5450) Polishing.

<http://dx.doi.org/10.1364/AO.54.010137>

1. INTRODUCTION

Mid-infrared (IR) light has been used extensively for astronomy, as well as for sensing, security, and military applications. It is known that refractive optical systems are not suitable for observations of mid-IR radiation from space, because of the large chromatic aberration caused by the dispersion of lens materials. Furthermore, there is no optical material that is suitable for an achromatic lens that covers the whole IR range of interest. In addition, refractive optics are not appropriate for large-sized astronomical observation systems because the optical mounts required to fix such heavy lens become fragile around cryogenic temperatures [1]. These issues can be solved by employing reflective optical systems. However, typical on-axis reflective telescopes, such as Cassegrain-type ones, have intrinsic deficiencies

caused by secondary mirror obstruction. The resultant stray light, scattering, and diffraction generate undesirable photon noise in observed optical signals [1–3].

In contrast, these problems do not exist in obstruction-free, off-axis reflective systems because the optical paths are all in free space and, thus, are not subject to obstruction. They can be applied to a payload on microsatellites or sounding rockets for wide-field mid-IR observations, e.g., diffuse interstellar media or cosmic background radiation in the mid- and far-IR wavelength regimes [4–7]. In addition, off-axis reflective systems can be adopted to a fore-optics system for ground-based astronomical IR spectrographs [8].

Although off-axis reflective telescopes are free from secondary obstruction issues, linear astigmatism can cause serious image degradation if they are not properly designed [9–12].

It was revealed that this linear astigmatism can be completely eliminated in a confocal off-axis reflecting telescope with a certain combination of mirror curvatures, distance between mirrors, and incident angles of the optical axis ray (OAR) based on a new geometrical aberration theory [9,10,13–15]. Applying this theory, we have developed a proto-model of a Schwarzschild–Chang type off-axis telescope, where a very wide field of view ($8.2^\circ \times 6.2^\circ$) can be realized with only two reflective mirrors. Figure 1 shows the side view of the telescope. The entrance pupil diameter (EPD) of this telescope is 50 mm and the focal ratio is 2 [16].

An off-axis mirror based on a conventional coaxial off-axis reflective system can be readily manufactured by cutting a small part of conic section from a large aspheric parent mirror. In this case, finding the optimum machining condition is relatively easy because the parent mirror is axially symmetric. However, this method is not applicable to our off-axis mirror case because the mirror is no longer a part of the axially symmetric parent mirror. From a machining point of view, its sophisticated surface should be created from a raw freeform mirror surface [17–19]. Thanks to the advances of single point diamond turning (SPDT) technology, freeform mirrors can be directly manufactured by an ultraprecision diamond turning machining process [20–24].

The spatial errors made on the optical surface are the primary factors determining the optical performance of the fabricated mirrors. These errors can be categorized into the following three subgroups [25–30].

(1) Low-frequency error (LFE) indicates how well the machined surface figure fits into its designed shape. It is represented by peak-to-valley (P-V) or root mean square (RMS) values. In the mid-IR range, the size of LFE is a few micrometers or less and is usually calculated by measuring the whole surface in spatial frequency of μm^{-1} .

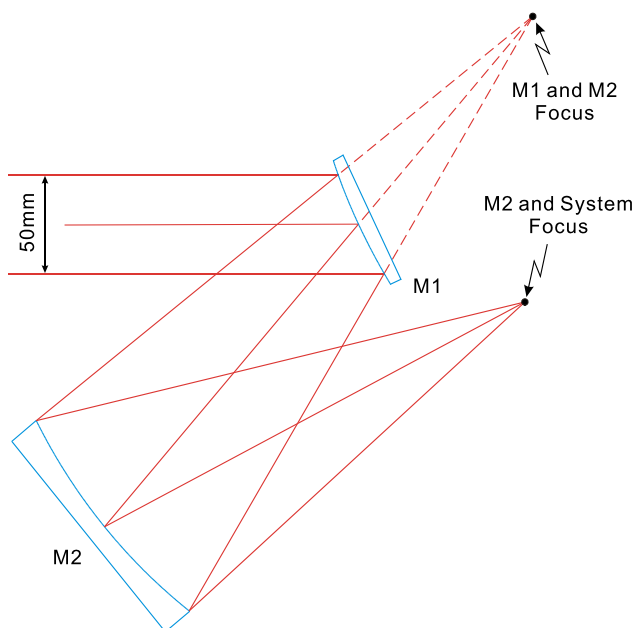


Fig. 1. Optical design of a Schwarzschild–Chang-type off-axis telescope. See the details of the design in [16].

(2) Mid-frequency error (MFE), commonly known as tool marks or turning marks, is the concentric ripples on the surface. The scale of MFE is tens of nanometers, which corresponds to tens of μm^{-1} in spatial frequency. This error originates from the spiral path of the diamond tool left on the turning material. The grating-like patterns produce diffraction and interference effects.

(3) High-frequency error (HFE) is described as the surface reflectivity and is responsible for loss of signal due to surface scattering. It is generally indicated via the central line averages of surface roughness (Ra) or RMS values of surface roughness (Rq) on a scale of the order of a few nanometers for local region of a few hundreds \times a few hundreds μm^2 in spatial frequency of nm^{-1} .

Among these errors, MFE can generally be removed by mechanical polishing after the SPDT process, but polishing of the soft surface of ductile aluminum is very difficult because the polishing process inevitably degrades the elaborate figure of the mirror surface. Many polishing techniques have been used to remove MFE, such as ion beam figuring (IBF), magneto-rheological finishing (MRF), abrasive or fluid jet polishing (AJP or FJP), computer-controlled optical surfacing (CCOS), and chemical mechanical polishing (CMP) [29,31–37]. These common polishing techniques use a thick (more than a hundred micrometers) electroless nickel plated aluminum mirror, except CMP, which is direct polishing of symmetric surfaces on bare aluminum [37–39]. However, these traditional methods are focused on the polishing technique for planar and aspheric mirrors; our paper will concentrate on the simple and effective procedure for an asymmetric freeform mirror.

In the case of a freeform surface, there are the challenges of using on-machine measurement and compensation machining. Because of that, in SPDT machining of a freeform surface, it is extremely difficult to find the optimum machining conditions during just a few repetitions. If SPDT machining is not finished during a few repetitions and the limited dimension of the nickel plating is consumed, the plating process must be repeated. As an attempt to avoid the repetition of plating and the limit of SPDT machining in a typical thick plating method, we suggest a novel thin plating procedure as explained in the following section. This procedure can repeat the SPDT machining without limit and this benefit allows simplification of the manufacturing procedure. Furthermore, this procedure also reduces the bimetallic effect and can be more stable than a traditional thick plating procedure [40].

In this paper, we propose and demonstrate a thin electroless nickel plating procedure to fabricate freeform mirrors. We will compare our procedure with typical methods used to make the freeform mirror of a Schwarzschild–Chang-type off-axis telescope and analyze the fabrication results. Because we concentrate on the practicality of the thin plating procedure, our experiment is performed only for the secondary mirror, which has a larger diameter than the primary mirror.

2. FABRICATION OF A FREEFORM MIRROR

A. SPDT Machining

We chose Al6061-T6 aluminum alloy for the material of the freeform mirrors and use a three-axis ultraprecision CNC

diamond turning lathe, Nanotech 450 UPL (Moore Nanotechnology Systems, USA) with a slow slide servo [41]. An aerostatic spindle (c axis) is used to rotate a mirror and an x-axis linear servo rotates on a hydrostatic bearing for lateral movement of the spindle. Also, a z-axis linear hydrostatic servo is controlled by a function of the x and c axes to generate a depth profile for an asymmetric surface. Rotation of the c axis is controlled at a low speed of about 50 RPM so that we can control the three axes to synchronize the spin of the c axis and the position of the diamond bite.

B. Electroless Nickel Plating and Baking

Several materials and methods can be used to improve the hardness of a mirror surface for the polishing process. We chose an electroless nickel plating that contains a few percent of phosphorus (hereafter Ni-P plating) on the aluminum (Al6061-T6) surface. In addition, we baked the Ni-P plated mirrors to increase the surface hardness. We also measured the relationship between hardness and baking time. The Ni-P plated samples were baked at 200°C with time duration of 0 (unbaked), 3, 6, 9, and 12 h. A micro-hardness tester, HM-122 (Mitutoyo, Japan) was used under conditions of a test force of 1961 mN with a load dwell time of 15 s. Figure 2 shows the hardness test results of the Ni-P plated mirror surfaces with different baking conditions. We measured five points for each mirror and derived the uncertainty of the measurements. The hardness of an Al-6061-T6 is approximately 80. The hardness of the mirror surface was increased more than 6 times by the Ni-P plating process. After the baking, the hardness was increased 5%–10% compared with the unbaked Ni-P plating aluminum surface (see Fig. 2). From the experiment, we conclude that 8–10 h baking time is suitable.

C. Sequences of Two Different Manufacturing Procedures

The flowchart in Fig. 3 shows sequences of two different procedures to fabricate the freeform mirrors and to remove MFE. The procedure along the left sequence is that commonly used in optical machining to manufacture a freeform mirror with a thick Ni-P plated (more than 100 micrometers in thickness) aluminum alloy [27,29,39]. First, the best fitted spherical surface of our freeform surface was fabricated with aluminum alloy. We performed the first SPDT process with rough

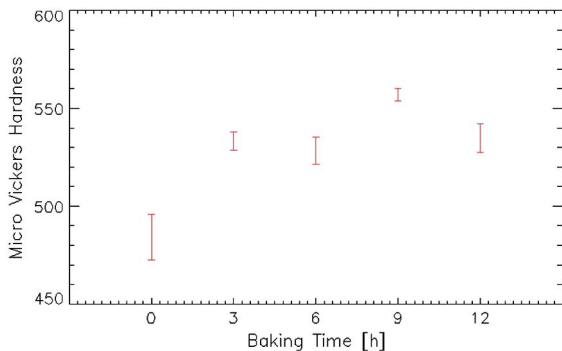


Fig. 2. Hardness measurement of Ni-P with different baking conditions.

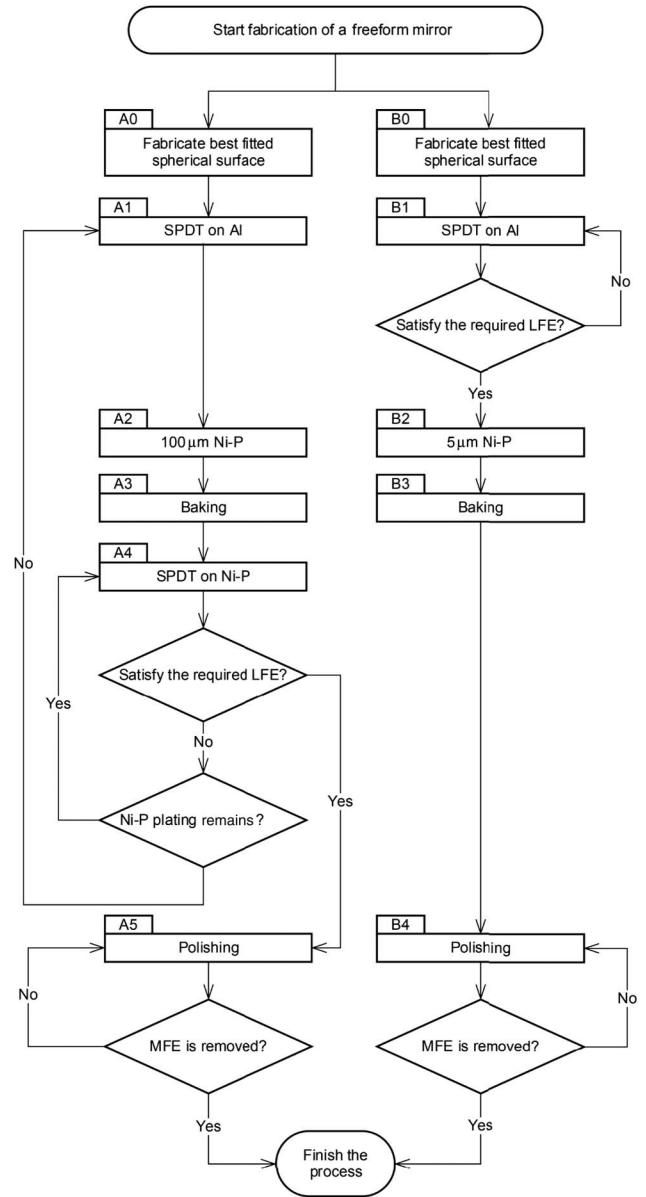


Fig. 3. Two different processes to remove MFE from an off-axis mirror. The surface measurement results at each process are listed in Table 1.

cutting because our mirror design has huge differences from the best fitted spherical surface, as shown in Fig. 4. After that, we plated Ni-P of 100 μm thickness on the diamond turned surface. At the second SPDT process, one rough cutting and several fine cuttings were executed to find the optimum cutting condition that satisfies the LFE tolerance limit. Finally, we performed polishing to remove MFE. However, this 100 μm procedure is not suitable for a freeform mirror. The minimum required cutting depths of SPDT processes are 20–30 μm for rough cutting and 5 μm for fine cutting. Different from flat, spherical, and aspheric surfaces, for which the compensation machining process can be used, machining of freeform surfaces is extremely difficult since it is hard to find the optimum machining conditions during just a few

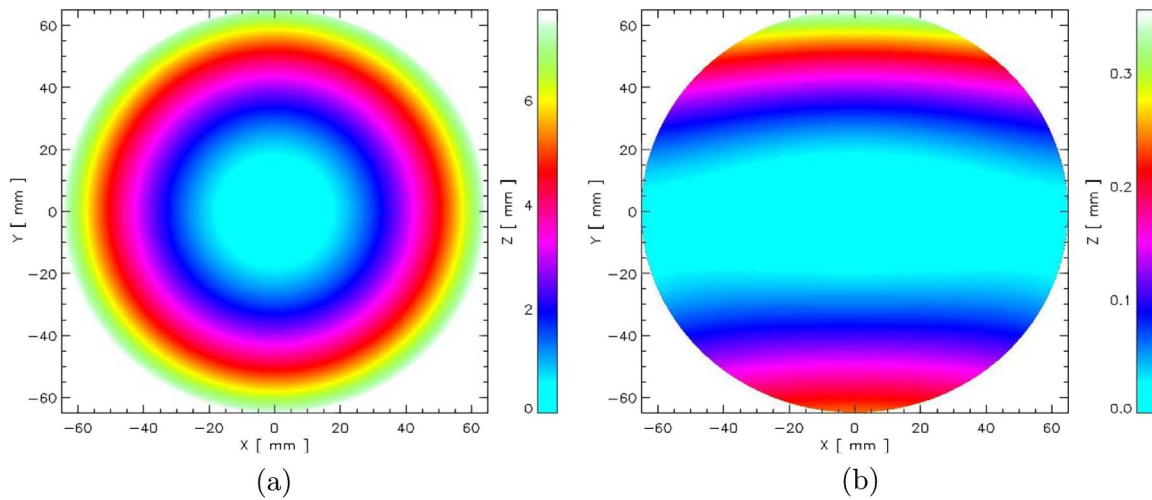


Fig. 4. Intensity map of the off-axis mirror. (a) Designed surface and (b) sag difference from the best fitted spherical surface.

machining processes. So, we should return back to the first SPDT process if the Ni-P plating is exhausted and the LFE does not satisfy the requirement. Furthermore, it is also difficult to plate very thick Ni-P.

For these reasons, we plated Ni-P of 5 μm thickness instead of the common thick Ni-P plating. This procedure is described on the right side of Fig. 3. This procedure also starts with the fabrication of the best fitted spherical surface of the freeform mirror. However, different from the 100 μm procedure, thin plating has little effect on the surface figure of the bare aluminum. Hence, SPDT machining on a bare aluminum surface can be repeated without limit until the desired surface figure is obtained. After the fine SPDT, we plated Ni-P on the aluminum surface with 5 μm thickness. Since the uniformity of thickness of the Ni-P plating is critical to keep the surface figure, we checked the change of LFE before and after the baking and polishing processes (see Section 3).

D. Manual Polishing of the Freeform Mirror

We applied a manual polishing technique with a commercial air polisher, abrasive material, and polishing pad. The size and the tilt angle of the polishing head are 17 mm and 45°, respectively. We used a metal polishing cream containing 25% of abrasive material. We performed first polishing with 200 RPM to remove the interference patterns on the mirror surface. After the first polishing, we performed fine polishing with 10,000 RPM.

3. MEASUREMENT

A. Contact-Type Measurement

During the SPDT, Ni-P plating, and polishing sequences, we checked the change of LFE and MFE using an ultrahigh accuracy 3D profilometer (UA3P, Panasonic Corp., Japan). UA3P measures a surface using an atomic force probe, which can measure the surfaces of any material without damage due to its low measuring pressure [42]. At each machining process, each mirror was measured on more than 1.7 million points with 1 μm pitch for accurate measurement and analysis. The

P-V and RMS values in Table 1 represent the measured LFE changes of the freeform mirrors.

We calculated the power spectrum density (PSD) to quantify the MFE of the freeform mirrors [29,43]. The fast Fourier transform (FFT) of a surface height, $H(f)$, is defined as

$$H(f) = \int_{-\frac{a}{2}}^{\frac{a}{2}} h(x)e^{-2\pi ifx} dx, \quad (1)$$

where a is the total width, x is the position of the surface, and $h(x)$ is the height at position x . Figure 5 shows the analysis results. The red line indicates the unpolished freeform mirror, while the blue and green lines are polished surfaces of the 100 and 5 μm procedures, respectively.

B. Noncontact-Type Measurement

The changes of MFE and HFE by the polishing process were also measured using NT 2000 (Wyko Inc., USA) which is a noncontact optical surface profilometer based on a Mirau interference microscope. The vertical resolution of this equipment is 0.1 nm [44]. Figure 6 shows the surface images of freeform mirrors obtained by the NT 2000. These images indicate the HFE values of a local region in Ra units, but we can also estimate the MFE patterns on the freeform surfaces. We

Table 1. Sequences of Two Different Manufacturing Procedures and Surface Measurements

	Process	P-V [μm]	RMS [μm]	Pit [%]
(A1)	Rough SPDT on Al	—	—	—
(A2)	Ni-P 100 μm	—	—	—
(A3)	Baking	—	—	—
(A4)	Fine SPDT on Ni-P	6.25	0.93	None
(A5)	Polishing	4.24	0.75	None
(B1)	Fine SPDT on Al	7.59	0.07	—
(B2)	Ni-P 5 μm	2.72	0.11	0.01
(B3)	Baking	7.55	0.12	0.09
(B4)	Polishing	1.80	0.08	0.01

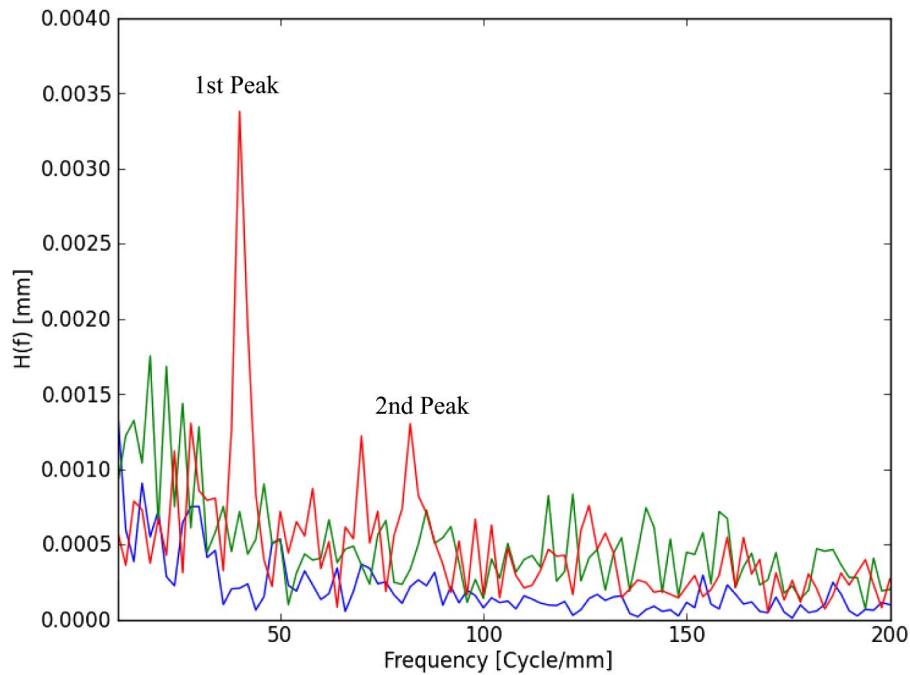


Fig. 5. PSD analysis results. The red line indicates the unpolished surface. Blue and green lines are the polished surfaces of the 100 and 5 μm procedures, respectively.

checked the change of MFE using the NT2000. However, we did not perform the PSD analysis using the data obtained from the NT2000 because it measures a more localized region of the mirror surface; it does not provide a large enough number of data points for PSD analysis. Before the polishing process, the SPDT marks on the mirror surface can be clearly seen in Fig. 6(a) and the Ra of the surface is 7.97 nm. Figures 6(b) and 6(c) show the surfaces of the 100 and 5 μm plating procedures, respectively. The Ra values of these surfaces are 3.9 nm (100 μm plating) and 13.5 nm (5 μm plating). We can find plenty of pits appearing in the polished surface of the 5 μm Ni-P plated mirror in Fig. 6(c).

C. Diffraction and Interference Pattern Test

The MFE around the center of the mirror is a rotationally symmetric signature, like concentric circles, while that at the edge of the mirror looks like a parallel grating [25]. In order to detect this grating pattern and estimate the size of the MFE using a simple grating equation, we checked the mirror region 25 mm away from its center with a visible light source (wavelength = 650 ± 5 nm). A pinhole and a neutral density filter, respectively, are used to obtain a Gaussian beam profile and a power level suitable for measurements. Figure 7 shows the schematic of the interference test. The angles of the incident (α) and reflected (β) ray are 33.48° and 20.62° , respectively. Also, the distances from laser to mirror and mirror to screen are 167 mm and 125 mm, respectively. If the MFE on the unpolished mirror works like a grating, we can estimate the width of the MFE by the following grating equation:

$$m\lambda = \sigma(\sin \alpha + \sin \beta), \quad (2)$$

where λ is the wavelength of light, m is the grating order, and σ is the groove density of the grating, which is consistent with the reciprocal of the width of the MFE. Also, α is the incident angle of the ray and β is the angle of the ray reflected by the grating. Figure 8 shows the interference test results.

4. RESULTS AND DISCUSSION

A. Change of LFE

The LFEs of the 100 and 5 μm Ni-P plating were measured using UA3P. As shown in Table 1, the LFE values of the free-form mirrors were measured in P-V and RMS values. The LFE of the 100 μm Ni-P plating mirror is very poor because the SPDT machining process of this procedure is limited by the thickness of the Ni-P plating. The LFE was slightly decreased during the polishing process, but it was too large to be compensated. In the case of the 5 μm procedure, P-V values change during processes. We expect that the change of the P-V value is attributed to the pits and nodules produced during the plating process. The P-V value appears to be improved after the plating, but this is because the pits and nodules occupy a very small area and, thus, were not detected during the UA3P measurement. Based on the measured RMS values, the change in LFE is negligible. Finally, as shown in Table 1, we confirmed that the RMS values for the two different procedures are enhanced or maintained during the entire process.

B. Change of MFE

The changes of MFE are verified by three different methods.

(1) PSD analysis using FFT of the UA3P measurement data. The red line in Fig. 5 indicates the PSD analysis result

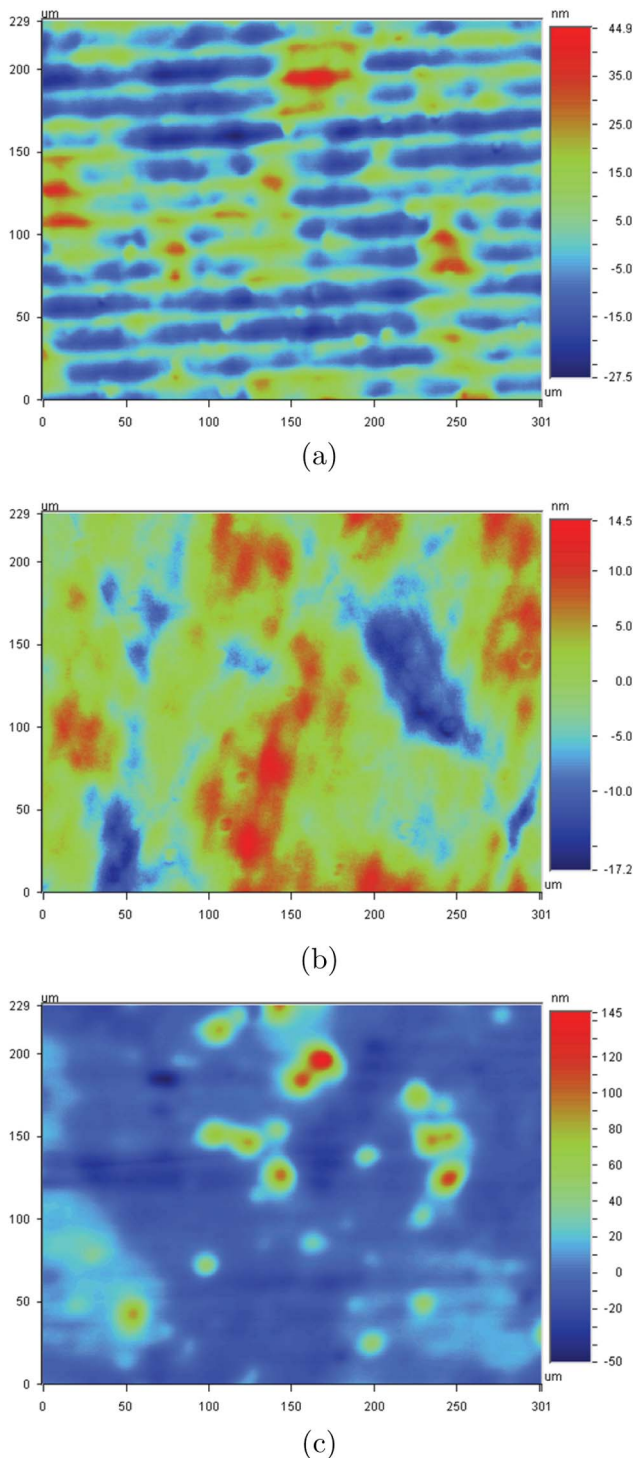


Fig. 6. MFE on the freeform mirror surface: (a) the unpolished surface with MFEs of width and depth of approximately 15–20 μm and 75 nm, respectively; (b) the 100 μm Ni-P plated polished surface; and (c) the 5 μm Ni-P plated polished surface.

of an unpolished freeform surface. The first peak in the red line indicates the period of 24 μm , which corresponds to the width of the MFE. The second peak is the harmonic frequency of the first one. The blue and the green lines are the PSD results of the polished mirrors of the 100 and 5 μm procedures,

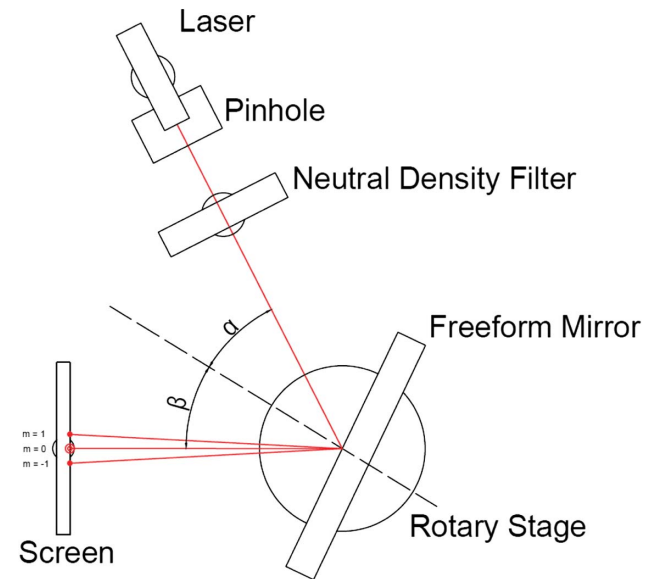


Fig. 7. Schematic of the interference test.

respectively. The peaks disappear and the PSD curves are slightly decreased by the polishing process. The PSD result shows the traditional 100 μm procedure has slightly less MFE than our 5 μm procedure after manual polishing. However, the disappearance of harmonic peaks in the PSD analysis results show that the MFE on the freeform mirror has been reduced significantly.

(2) Evaluation of the randomization of the SPDT marks on the freeform surfaces by the NT 2000. Although minute MFEs remain on the surface in Fig. 6(c), they are significantly diminished and seem to be mostly randomized as compared with Fig. 6(a). We ascertain that SPDT marks are mostly changed to the randomized patterns by the polishing process, as shown in Fig. 6.

(3) Measuring diffraction and interference patterns by optical test. The distances of interference patterns in Fig. 8(a) are 5.06 and 5.12 mm for grating orders of $m = +1$ and $m = -1$, respectively. The estimated widths of the MFE are 19.01 μm and 19.30 μm , respectively. However, as shown in Figs. 8(b) and 8(c), the $m \pm 1$ order grating-like patterns disappeared.

The estimated MFE value of the PSD analysis result is not exactly consistent with the interference test. However, both of them are in the range of the measurement result of the NT 2000 shown in Fig. 6(a). Finally, we confirmed that the MFE on the freeform mirror surfaces were successfully removed and LFEs were maintained for both procedures.

C. Change of HFE

The changes of HFE were checked using NT2000. The HFE of the 100 μm Ni-P plated freeform mirror was decreased. Although the HFE of the 5 μm plating is slightly increased by the pits on the surface which seems to be attributed to the Ni-P plating process, it is a tiny parts (less than 0.1%) of the whole surface and does not seem to affect optical performance. We expect this problem can be solved by adding a filtering equipment to plating process.

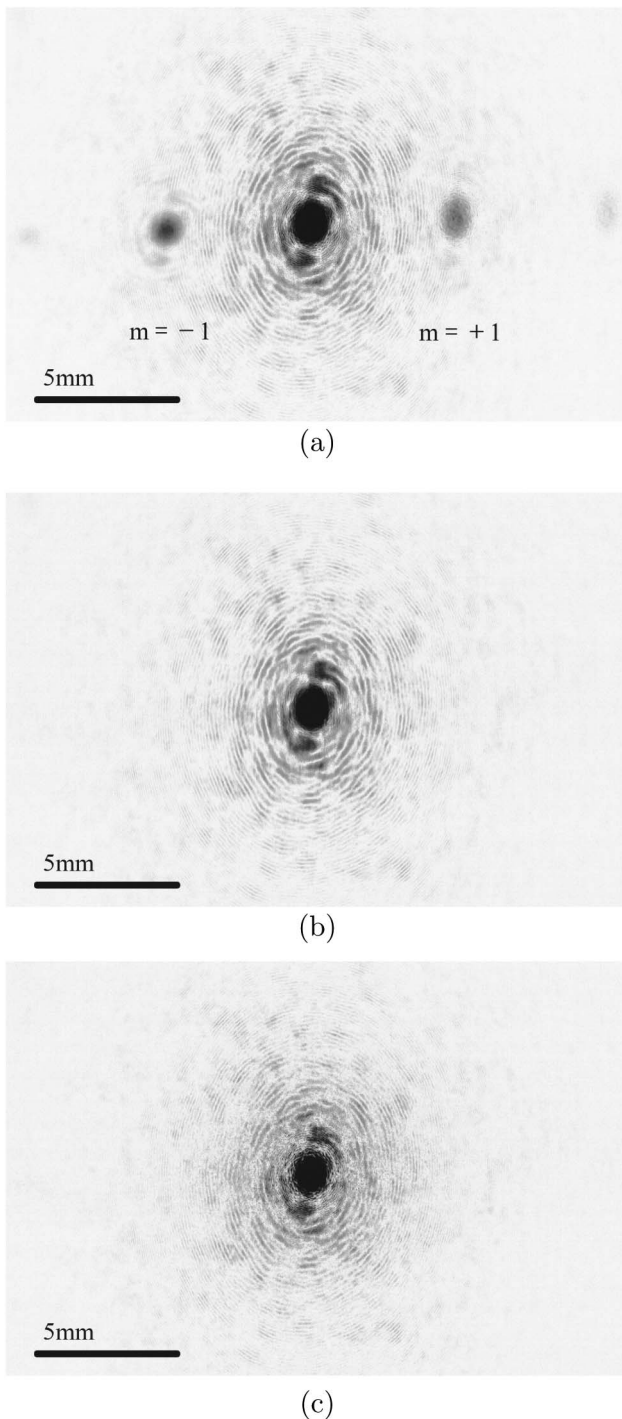


Fig. 8. Interference test result: (a) grating-like pattern created by MFEs on the unpolished surface, (b) the 100 μm Ni-P plated polished surface, and (c) the 5 μm Ni-P plated polished surface.

5. CONCLUSION

In conclusion, we have proposed and demonstrated a thin electroless nickel plating procedure to remove MFEs from freeform mirrors. Compared with the typical method, this procedure has the advantages of a simplified sequence and unlimited SPDT machining. In our experiments, freeform mirrors were manufactured by two different procedures, and we confirmed the

practicality of our suggestion. We have verified the fabrication results by three different kinds of methods:

- (1) The LFE and MFE have been checked by contact type measurement.
- (2) The MFE and HFE have been monitored by noncontact-type measurement.
- (3) The diffraction and interference patterns that are generated by MFEs have been checked by an optical test.

We ascertained that LFEs are maintained during the entire process in both procedures.

The traditional procedure has an advantage in precision machining of symmetric surfaces because, in this case, there is no plating uniformity issue that is sensitively influenced by pits and nodules. However, the freeform mirror that was fabricated by the typical procedure did not satisfy LFE requirement due to the limitation of SPDT machining. The three different kinds of experimental results indicate that the MFEs on the mirrors have been removed and randomized. As a result of the typical thick plating procedure, the HFE was decreased. Although the HFE of thin plating is slightly increased by pitting, the proportion of this is less than 0.1% of the whole surface and does not seem to affect the optical performance in the mid-IR wavelength range. The results show that the proposed thin plating procedure can be a simple but effective solution to remove the MFE on freeform mirrors for mid-IR applications. We highlight that this proposed method can be of help in developing a freeform mirror for a confocal off-axis system that provides a wide field of view with zero chromatic aberration, no obstruction, and no linear astigmatism.

Funding. Ministry of Education of Korea (BK21 plus program); National Research Foundation of Korea (NRF) (NRF-2014M1A3A3A02034810).

REFERENCES

1. Y. H. Lee, "Alignment of an off-axis parabolic mirror with two parallel He-Ne laser beams," *Opt. Eng.* **31**, 2287–2292 (1992).
2. J. R. Kuhn and S. L. Hawley, "Some astronomical performance advantages of off-axis telescopes," *Publ. Astron. Soc. Pac.* **111**, 601–620 (1999).
3. J. R. Kuhn and G. Moretto, "Wide-field off-axis new planetary telescope," *Proc. SPIE* **4003**, 324–330 (2000).
4. J. Bock, J. Battle, A. Cooray, M. Kawada, B. Keating, A. Lange, D.-H. Lee, T. Matsumoto, S. Matsuura, S. Pak, T. Renbarger, I. Sullivan, K. Tsumura, T. Wada, and T. Watabe, "The cosmic infrared background experiment," *New Astron. Rev.* **50**, 215–220 (2006).
5. D.-H. Lee, S. Pak, I.-S. Yuk, U.-W. Nam, H. Jin, S. Lee, J.-W. Han, H. Yang, D. L. Kim, G.-H. Kim, S.-J. Park, B.-H. Kim, and H. Jeong, "Design of the optical system for a protomodel of space infrared cryogenic system," *J. Astron. Space Sci.* **22**, 473–482 (2005).
6. I.-S. Yuk, H. Jin, S. Lee, Y.-S. Park, D.-H. Lee, U.-W. Nam, J.-H. Park, W.-Y. Han, and J.-W. Lee, "Preliminary optical design of MIRIS, main payload of STSAT-3," *Publ. Korean Astron. Soc.* **22**, 201–209 (2007).
7. W.-S. Jeong, S.-J. Park, K. Park, D.-H. Lee, J. Pyo, B. Mon, Y. Park, I.-J. Kim, W.-K. Park, D.-H. Lee, C. Park, K. Ko, T. Matsumoto, N. Takeyama, A. Enokuchi, G.-W. Shin, J. Chae, and U.-W. Nam, "Conceptual design of the NISS onboard NEXTSat-1," *J. Astron. Space Sci.* **31**, 83–90 (2014).
8. C. Park, D. T. Jaffe, I.-S. Yuk, M.-Y. Chun, S. Pak, K.-M. Kim, M. Pavel, H. Lee, H. Oh, U. Jeong, C. K. Sim, H.-I. Lee, H. A. Nguyen Le, J. Strubhar, M. Gully-Santiago, J. S. Oh, S.-M. Cha, B. Moon,

- K. Park, C. Brooks, K. Ko, J.-Y. Han, J. Nah, P. C. Hill, S. Lee, S. Barnes, Y. S. Yu, K. Kaplan, G. Mace, H. Kim, J.-J. Lee, N. Hwang, and B.-G. Park, "Design and early performance of IGRINS (immersion grating infrared spectrometer)," *Proc. SPIE* **9147**, 91471D (2014).
9. S. Chang, "Geometrical theory of aberrations for classical offset reflector antennas and telescopes," Ph.D. thesis (University of Southern California, 2003).
 10. S. Chang, "Off-axis reflecting telescope with axially-symmetric optical property and its applications," *Proc. SPIE* **6265**, 626548 (2006).
 11. G. Moretto and J. R. Kuhn, "Optical performance of the 6.5-m off-axis new planetary telescope," *Appl. Opt.* **39**, 2782–2789 (2000).
 12. G. Moretto, M. Langlois, and M. Ferrari, "Suitable off-axis space-based telescope designs," *Proc. SPIE* **5487**, 1111–1118 (2004).
 13. S. Chang and A. Prata, Jr., "Geometrical theory of aberrations near the axis in classical off-axis reflecting telescopes," *J. Opt. Soc. Am. A* **22**, 2454–2464 (2005).
 14. S. Chang, J. H. Lee, S. P. Kim, H. Kim, W. J. Kim, I. Song, and W. Park, "Linear astigmatism of confocal off-axis reflective imaging systems and its elimination," *Appl. Opt.* **45**, 484–488 (2006).
 15. S. Chang, "Elimination of linear astigmatism in off-axis three-mirror telescope and its applications," *Proc. SPIE* **8860**, 88600U (2013).
 16. S. Kim, S. Pak, S. Chang, G. H. Kim, S. C. Yang, M. S. Kim, S. Lee, and H. Lee, "Proto-model of an infrared wide-field off-axis telescope," *J. Korean Astron. Soc.* **43**, 169–181 (2010).
 17. F. Z. Fang, X. D. Zhang, A. Weckenmann, G. X. Zhang, and C. Evans, "Manufacturing and measurement of freeform optics," *CIRP Ann.* **62**, 823–846 (2013).
 18. C. J. Evans and J. B. Bryan, "Structured, textured or engineered surfaces," *CIRP Ann.* **48**, 541–556 (1999).
 19. K. Garrard, T. Bruegge, J. Hoffman, T. Dow, and A. Sohn, "Design tools for freeform optics," *Proc. SPIE* **5874**, 95–105 (2005).
 20. L. Li, X. Min, D. Chen, and J. Wang, "Special techniques in ultra-precision machining," *Proc. SPIE* **6722**, 672213 (2007).
 21. C. F. Cheung, L. B. Kong, and M. J. Ren, "Measurement and characterization of ultra-precision freeform surfaces using an intrinsic surface feature-based method," *Meas. Sci. Technol.* **21**, 115109 (2010).
 22. C. F. Cheung, K. Hu, X. Q. Jiang, and L. B. Kong, "Characterization of surface defects of structured freeform surfaces using a pattern recognition and analysis method," *Meas. Sci. Technol.* **43**, 1240–1249 (2010).
 23. G. H. Kim, S. C. Yang, H. S. Kim, I. J. Lee, M. H. Kook, and D. Lee, "Ultra precision machining technology of infrared optical system for astronomy and space," *J. Korean Soc. Precis. Eng.* **24**, 25–32 (2007).
 24. S. C. Yang, G. H. Kim, H. S. Kim, S. Y. Lee, M. S. Kim, and J. H. Won, "Ultra precision machining technology of infrared optical system for aerospace," *J. Korean Soc. Precis. Eng.* **24**, 19–24 (2007).
 25. J. M. Tamkin, W. J. Dallas, and T. D. Milster, "Theory of point-spread function artifacts due to mid-spatial frequency surface errors," *Appl. Opt.* **49**, 4814–4824 (2010).
 26. J. M. Tamkin, T. D. Milster, and W. J. Dallas, "Theory of modulation transfer function artifacts due to mid-spatial-frequency errors and its application to optical tolerancing," *Appl. Opt.* **49**, 4825–4835 (2010).
 27. A. Beaucamp, R. Freeman, R. Morton, K. Ponudurai, and D. D. Walker, "Removal of diamond-turning signatures on x-ray mandrels and metal optics by fluid-jet polishing," *Proc. SPIE* **7018**, 701835 (2008).
 28. R. J. Noll, "Effect of mid- and high-spatial frequencies on optical performance," *Opt. Eng.* **18**, 182137 (1979).
 29. Z. Z. Li, J. M. Wang, X. Q. Peng, L. T. Ho, Z. Q. Yin, S. Y. Li, and C. F. Cheung, "Removal of single point diamond-turning marks by abrasive jet polishing," *Appl. Opt.* **50**, 2458–2463 (2011).
 30. R. C. Juergens, *Fundamentals of Optical Engineering* (Raytheon Missile Systems, 2005).
 31. A. Shorey, W. Kordonski, and M. Tricard, "Magnetorheological finishing of large and lightweight optics," *Proc. SPIE* **5533**, 99–107 (2004).
 32. C. J. Jiao, S. Y. Li, and X. H. Xie, "Algorithm for ion beam figuring of low-gradient mirrors," *Appl. Opt.* **48**, 4090–4096 (2009).
 33. O. W. Föhnle, H. V. Brug, and H. J. Frankena, "Fluid jet polishing of optical surfaces," *Appl. Opt.* **37**, 6771–6773 (1998).
 34. D. W. Kim, S.-W. Kim, and J. H. Burge, "Non-sequential optimization technique for a computer controlled optical surfacing process using multiple tool influence functions," *Opt. Express* **17**, 21850–21866 (2009).
 35. S. M. Booi, H. V. Brug, J. J. M. Braat, and O. W. Föhnle, "Nanometer deep shaping with fluid jet polishing," *Opt. Eng.* **41**, 1926–1931 (2002).
 36. Z. Z. Li, S. Y. Li, Y. F. Dai, and X. Q. Peng, "Optimization and application of influence function in abrasive jet polishing," *Appl. Opt.* **49**, 2947–2953 (2010).
 37. Z. Yin and Z. Yi, "Direct polishing of aluminum mirrors with higher quality and accuracy," *Appl. Opt.* **54**, 7835–7841 (2015).
 38. K. S. Chon and Y. Namba, "Single-point diamond turning of electroless nickel for flat x-ray mirror," *J. Mech. Sci. Technol.* **24**, 1603–1609 (2010).
 39. A. Beaucamp and Y. Namba, "Super-smooth finishing of diamond turned hard x-ray molding dies by combined fluid jet and bonnet polishing," *CIRP Ann.* **62**, 315–318 (2013).
 40. J. Kinast, M. Beier, A. Gebhardt, S. Risse, and A. Tünnermann, "Polishability of thin electrolytic and electroless NiP layers," *Proc. SPIE* **9633**, 963311 (2015).
 41. Y. Tohme and R. Murray, *Principles and Applications of the Slow Slide Servo* (Moore Nanotechnology Systems, 2005).
 42. H. Tsutsumi, K. Yoshizumi, and H. Takeuchi, "Ultrahigh accurate 3D profilometer," *Proc. SPIE* **5638**, 387–394 (2005).
 43. E. Sidick, "Power spectral density specification and analysis of large optical surfaces," *Proc. SPIE* **7390**, 73900L (2009).
 44. J. C. Wyant, "White light interferometry," *Proc. SPIE* **4737**, 98–107 (2002).